Exact and asymptotic Green functions in homogeneous anisotropic viscoelastic media

Václav Vavryčuk

Geophysical Institute, Academy of Sciences of the Czech Republic, Boční II/1401, Praha 4, Czech Republic, E-mail: vv@ig.cas.cz

ABSTRACT

An asymptotic Green function in homogeneous anisotropic viscoelastic media is derived. The Green function in viscoelastic media is formally similar to that in elastic media, but its computation is more involved. The stationary slowness vector is, in general, complex-valued and inhomogeneous. Its computation involves finding two independent real-valued unit vectors which specify the directions of its real and imaginary parts and can be done either by iterations or by solving a system of coupled polynomial equations. When the stationary slowness direction is found, all quantities standing in the Green function such as the slowness vector, polarization vector, phase and energy velocities, and principal curvatures of the slowness surface can readily be calculated.

The formulas for the exact and asymptotic Green functions are numerically checked against closed-form solutions for isotropic and simple anisotropic, elastic and viscoelastic models. The calculations confirm that the formulas and developed numerical codes are correct. The computation of the *P*-wave Green function in two realistic materials with a rather strong anisotropy and absorption indicates that the asymptotic Green function is accurate at distances greater than several wavelengths from the source. The error in the modulus reaches at most 4% at distances greater than 15 wavelengths from the source.

1. INTRODUCTION

Theory od waves propagating in viscoelastic media becomes increasingly important and intensively developed in recent years (Auld 1973; Caviglia & Morro 1992; Carcione 2001). This concerns, studying the basic attributes of homogeneous and inhomogeneous plane waves such as slowness and attenuation vectors (Červený & Pšenčík 2005), deriving formulas for linearized attenuation coefficients (Zhu & Tsvankin 2006, 2007), studying acoustic axes (Shuvalov & Scott 1999; Shuvalov 2001), energy flux (Carcione & Cavallini 1993; Deschamps *et al.* 1997; Boulanger 1998; Červený & Pšenčík 2006), and reflection/transmission coefficients at a plane interface between two homogeneous viscoelastic halfspaces (Borcherdt 1977, 1982; Krebes 1983; Richards 1984; Wennerberg 1985; Nechtschein & Hron 1996; Brokešová 2001; Daley & Krebes 2004). In contrast to plane-wave propagation, considerably less attention has been paid to theory of waves excited by point or finite sources in isotropic and anisotropic viscoelastic media (Carcione 1994, 2001). So far, such wave fields are usually computed using numerical methods which directly solve the wave equation (Carcione 1990; Saenger & Bohlen 2004; Moczo *et al.* 2007).

In this paper, I study waves generated by point sources. I generalize the formula for the exact Green function in homogeneous anisotropic elastic media (Buchwald 1959; Burridge 1967; Willis 1980; Norris, 1994; Wang and Achenbach, 1994) to viscoelastic media. I present closed-form solutions of the exact viscoelastic Green function for isotropy and for three simple types of anisotropy. Further, I derive the asymptotic Green function valid for high-frequency signals at distances far from the source. I define wave fronts and other asymptotic quantities such as ray velocity and ray attenuation. In numerical modeling, I verify the correctness of the analytical, exact numerical, and asymptotic Green functions, and demonstrate their accuracy and efficiency.

In the next, real and imaginary parts of complex-valued quantities are denoted by superscripts *R* and *I*, respectively. A complex-conjugate quantity is denoted by an asterisk. The vector direction of a complex-valued vector $\mathbf{v}$ is calculated as $\mathbf{v}/\sqrt{\mathbf{v}\cdot\mathbf{v}}$ (the normalization condition $\mathbf{v}/\sqrt{\mathbf{v}\cdot\mathbf{v}^*}$ is not used, because it complicates generalizing some of real-valued equations to complex-valued ones). If any complex-valued vector is defined by a real-valued direction, it is called homogeneous, and if defined by a complex-valued

direction, it is called inhomogeneous. In formulas, the Einstein summation convention is used for repeated subscripts.

2. ANISOTROPIC VISCOELASTIC MEDIUM

Let us assume a time-harmonic plane wave described by the displacement vector

$$u_i(\mathrm{x},t) = U(\mathrm{x}) g_i \exp[-i\omega(t - \mathrm{p}\cdot\mathrm{x})] \,, \tag{1}$$

where x is the position vector, U the amplitude, g the unit polarization vector, ω the circular frequency, and t is time. Vector p is the slowness vector defined as $\mathrm{p} = \mathrm{n}/c$, where n is the slowness direction, and c the phase velocity. The plane wave propagates in the viscoelastic medium defined by the following stress-strain relation:

$$\sigma_{ij} = c^R_{ijkl} e_{kl} + \eta_{ijkl} \dot{e}_{kl} \,, \tag{2}$$

where σ_{ij} are the components of the stress tensor, e_{kl} the components of the strain tensor, $\dot{e}_{kl}$ is the time derivative of e_{kl}, and c^R_{ijkl} and η_{ijkl} are the components of the elasticity and viscosity tensors. These tensors must be positive definite to ensure that strain energy W and dissipation energy rate R are positive:

$$W = \frac{1}{2} c^R_{ijkl} e_{ij} e_{kl} > 0 \,,\; R = \frac{1}{2} \eta_{ijkl} \dot{e}_{ij} \dot{e}_{kl} > 0 \,. \tag{3}$$

Taking into account that $\dot{e}_{kl}$ is expressed for the time-harmonic wave (1) as

$$\dot{e}_{kl} = -i\omega \, e_{kl} \,, \tag{4}$$

stress-strain relation (2) can be formally written in a form identical with that for elastic media, where the real-valued elasticity tensor c^R_{ijkl} is substituted by the complex-valued frequency-dependent viscoelasticity tensor c_{ijkl},

$$c_{ijkl} = c^R_{ijkl} - i\omega\eta_{ijkl} \ . \tag{5}$$

This tensor is used to construct the complex-valued density-normalized viscoelasticty tensor $a_{ijkl} = c_{ijkl} / \rho$, and subsequently the complex-valued Christoffel tensor Γ_{jk}, defined alternatively in terms of slowness direction n,

$$\Gamma_{jk}(\mathrm{n}) = a_{ijkl} n_i n_l , \tag{6}$$

or slowness vector p,

$$\Gamma_{jk}(\mathrm{p}) = a_{ijkl} p_i p_l \ . \tag{7}$$

Slowness direction n is real-valued for homogeneous waves but complex-valued for inhomogeneous waves.

The Christoffel tensor Γ_{jk} has three eigenvalues and three eigenvectors, which define the properties of three plane waves propagating in anisotropic media. Eigenvalues $G(\mathrm{n})$ and $G(\mathrm{p})$ read

$$G(\mathrm{n}) = a_{ijkl} n_i n_l g_j g_k = c^2 , \tag{8}$$

$$G(\mathrm{p}) = a_{ijkl} p_i p_l g_j g_k = 1 \ , \tag{9}$$

and define phase velocity c and slowness vector p as a function of slowness direction n. The eigenvectors define polarization vectors g. The polarization vectors are normalized, so that $\mathrm{g} \cdot \mathrm{g} = 1$. Note that when applying condition $\mathrm{g} \cdot \mathrm{g}^* = 1$, equations (8) and (9) would have a different form containing also complex-conjugate quantities.

Using eigenvalue $G(\mathrm{p})$ we define the energy velocity vector as

$$v_i = \frac{1}{2}\frac{\partial G}{\partial p_i} = a_{ijkl} p_l g_j g_k \ , \tag{10}$$

which is called the group velocity vector in elastic media. Vectors v and p are related by the equation, $\mathrm{v}\cdot\mathrm{p} = 1$. The slowness vector, phase velocity, energy velocity and the polarization vectors are in general complex-valued.

3. EXACT GREEN FUNCTION

3.1. Elastic medium

The exact elastodynamic Green function in unbounded, homogeneous, anisotropic perfectly elastic media can be expressed in the frequency domain as the sum of regular and singular terms, $G_{kl}^{\mathrm{r}}(\mathrm{x},\omega)$ and $G_{kl}^{\mathrm{s}}(\mathrm{x},\omega)$, as follows (Burridge 1967; Willis 1980; Norris, 1994, Eq. 3.22; Wang and Achenbach, 1994, Eqs. 17-21):

$$G_{kl}^{\mathrm{exact}}(\mathrm{x},\omega) = G_{kl}^{\mathrm{r}}(\mathrm{x},\omega) + G_{kl}^{\mathrm{s}}(\mathrm{x}), \tag{11}$$

$$G_{kl}^{\mathrm{r}}(\mathrm{x},\omega) = \frac{i\omega}{8\pi^2\rho}\sum_{M=1}^{3}\int_{\substack{S(\mathrm{n})\\ \mathrm{n}\cdot\mathrm{x}>0}} \frac{g_k^{(M)} g_l^{(M)}}{\left(c^{(M)}\right)^3}\exp\left(i\omega\frac{\mathrm{n}\cdot\mathrm{x}}{c^{(M)}}\right) dS(\mathrm{n}) \ , \tag{12}$$

$$G_{kl}^{\mathrm{s}}(\mathrm{x}) = \frac{1}{8\pi^2\rho}\sum_{M=1}^{3}\int_{S(\mathrm{n})} \frac{g_k^{(M)} g_l^{(M)}}{\left(c^{(M)}\right)^2}\delta(\mathrm{n}\cdot\mathrm{x})\, dS(\mathrm{n}) \ . \tag{13}$$

Superscript M = 1,2,3 denotes the type of wave (P, $S1$ and $S2$), g = g(n) is the unit polarization vector, $c = c(\mathrm{n})$ is the phase velocity, ρ is the density of the medium, ω is the circular frequency, x = Nr is the position vector, r is the distance of the observation point from the source, N is the ray vector, n is the slowness direction, and S(n) is the unit sphere.

The regular term is integrated over a hemisphere, defined by $\mathrm{n}\cdot\mathrm{x}>0$. The singular term is integrated over a unit circle defined by $\mathrm{n}\cdot\mathrm{x}=0$. The reduction of the surface integral to a line integral in the singular term is due to the Dirac delta function $\delta(\mathrm{n}\cdot\mathrm{x})$ in the integrand. Since the singular term does not depend on frequency ω, it physically corresponds to the static Green function.

All quantities in (11-13) are real-valued including slowness direction n. Hence the regular part of the exact Green function is calculated as a superposition of homogeneous plane waves. This is the essential advantage of formulas (11-13) compared to other formulas for the Green function which involve also inhomogeneous waves specified by a complex-valued slowness direction n (e.g., the Green function in isotropic media calculated using the Weyl integral, see Aki & Richards, 2002, Sec. 6.1).

Formulas (11-13) can be derived in several alternative ways. Probably, the most straightforward way is to solve the elastodynamic equation in the slowness-frequency domain to obtain $G_{kl}(\mathrm{p},\omega)$. Subsequently $G_{kl}(\mathrm{x},\omega)$ is calculated by applying the inverse 3-D Fourier transform (see Mura 1987; Norris 1994; Červený 2001), which physically corresponds to a superposition of homogeneous plane waves propagating in an arbitrary direction with an arbitrary phase velocity. Using the residuum theorem, the 3-D integral is further reduced to a surface integral representing a superposition of homogeneous plane waves propagating in an arbitrary direction but with the phase velocity satisfying equation (8).

The integration in (12) and (13) can also be performed over slowness surface $S(\mathrm{p})$. Taking into account the relation between surface elements $dS(\mathrm{n})$ and $dS(\mathrm{p})$ (see Burridge 1967):

$$\mathrm{n}\cdot\mathrm{N}\,dS(\mathrm{p})=p^2 dS(\mathrm{n}), \tag{14}$$

and the relation between the phase and energy velocities c and v,

$$\mathrm{n}\cdot\mathrm{N}=\frac{c}{v}, \tag{15}$$

we can put for a particular wave (*P*, *S*1 or *S*2)

$$G_{kl}^{\mathrm{r}}(\mathrm{x},\omega)=\frac{i\omega}{8\pi^2\rho}\int\limits_{\substack{S(\mathrm{p})\\ \mathrm{p}\cdot\mathrm{x}>0}}\frac{g_k g_l}{v}\exp(i\omega\mathrm{p}\cdot\mathrm{x})\,dS(\mathrm{p})\,, \tag{16}$$

$$G_{kl}^{\mathrm{s}}(\mathrm{x})=\frac{1}{8\pi^2\rho}\int\limits_{S(\mathrm{p})}\frac{g_k g_l}{v}\delta(\mathrm{p}\cdot\mathrm{x})\,dS(\mathrm{p})\,. \tag{17}$$

The complete Green function is then a sum of contributions for all three waves.

3.2. Viscoelastic medium

The Green function in viscoelastic media is derived in a quite analogous way as in elastic media. The Green function is calculated by applying the inverse 3-D Fourier transform, which physically corresponds to a superposition of homogeneous plane waves propagating in an arbitrary direction with an arbitrary (real-valued) phase velocity. Using the residuum theorem, the 3-D integral is reduced to a surface integral representing a superposition of homogeneous plane waves propagating in an arbitrary direction but with complex-valued velocities satisfying equation (8) and with polarization vectors satisfying the Christoffel equation. Hence, the Green function is expressed by exactly the same formulas as formulas (11-13) and (16-17) derived for elastic media. The only difference is that some quantities in the integrands become complex-valued and frequency-dependent. This concerns phase velocity c, slowness vector p, energy velocity v, and polarization vector g. Slowness direction n, ray direction N, position vector x, and density ρ remain real-valued and do not depend on real-valued frequency ω.

Emphasize that p is a homogeneous complex-valued vector, hence its direction n in (11-13) remains real-valued. This is in agreement with the above statement that the exact Green function in viscoelastic media is calculated as a superposition of homogeneous plane waves similarly as in elastic media.

4. ASYMPTOTIC GREEN FUNCTION

Since the exact Green function is expressed in terms of complicated integrals, it is advantageous to evaluate the Green function asymptotically. Physically, it corresponds to studying the high-frequency Green function in the far field, i.e. at distances far from the source with respect to the predominant wavelength of the wave field. The asymptotic Green function significantly simplifies, because the singular term (17) is negligible, and integral (16) can be calculated using the stationary phase method for the elastic medium or the steepest descent method for the viscoelastic medium.

4.1. Elastic medium

Formula (16) can also be expressed as

$$G_{kl}^{\mathrm{r}}(\mathrm{x},\omega)=\frac{i\omega}{8\pi^2\rho}\int\limits_{\substack{S(\mathrm{p})\\ \theta(\mathrm{p})>0}} P_{kl}(\mathrm{p})\exp(i\lambda\theta(\mathrm{p}))dS(\mathrm{p})\ , \tag{18}$$

where

$$P_{kl}(\mathrm{p})=\frac{g_k(\mathrm{p})g_l(\mathrm{p})}{v(\mathrm{p})}\ \text{and}\ \ \theta(\mathrm{p})=\mathrm{p}\cdot\mathrm{N}\ . \tag{19}$$

Functions $P_{kl}(\mathrm{p})$ and $\theta(\mathrm{p})$ are assumed to be smooth, and parameter $\lambda=\omega r$ is large and positive. Phase $\theta(\mathrm{p})$ is positive inside the integration area and zero at its boundary. Expanding phase function $\theta(\mathrm{p})$ near stationary point p_0, defined by

$$\left.\frac{\partial\theta(\mathrm{p})}{\partial s_1}\right|_{\mathrm{p}=\mathrm{p}_0}=0\,,\quad \left.\frac{\partial\theta(\mathrm{p})}{\partial s_2}\right|_{\mathrm{p}=\mathrm{p}_0}=0\ , \tag{20}$$

yields

$$\theta(\mathrm{p}) = \mathrm{p}_0 \cdot \mathrm{N} - \frac{1}{2}\left(K_1 s_1^2 + K_2 s_2^2\right), \tag{21}$$

where K_1 and K_2 are the principal curvatures of the slowness surface at p_0, and s_1 and s_2 are the local coordinates defined on the slowness surface. The coordinate axes have their origin at p_0 and point along the principal curvatures of the slowness surface at p_0. The third coordinate axis s_3 is normal to the slowness surface at p_0 and parallel to N.

Applying the stationary phase method to integral (18), we obtain the asymptotic Green function $G_{kl}^{\mathrm{asym}}(\mathrm{x},\omega)$ in the following form (Buchwald 1959; Burridge 1967; Every & Kim 1994, Červený 2001, eq. 2.5.75)

$$G_{kl}^{\mathrm{asym}}(\mathrm{x},\omega) = \frac{1}{4\pi\rho}\,\frac{g_k g_l}{v\sqrt{|K|}}\,\frac{1}{r}\,\exp\left(i\frac{\pi}{2}\sigma_0 + i\omega\,\mathrm{p}_0 \cdot \mathrm{x}\right), \tag{22}$$

where $K = K_1 K_2$ is the Gaussian curvature of the slowness surface, and σ_0 is defined as

$$\sigma_0 = 1 - \frac{1}{2}\operatorname{sgn} K_1 - \frac{1}{2}\operatorname{sgn} K_2 \ . \tag{23}$$

Principal curvatures K_1 and K_2 are both positive for a convex surface, negative for a concave surface, and of opposite signs for a saddle-shaped surface. All quantities dependent on p in (22) are taken at stationary point p_0. Formula (22) works for all directions except for singularities, in which a more involved approach is required (Vavryčuk 1999, 2002; Gridin 2000).

4.2. Viscoelastic medium

Since phase velocity c is complex-valued in viscoelastic media, the slowness vector p and functions $P_{kl}(\mathrm{p})$ and $\theta(\mathrm{p})$ in (18) are also complex-valued. Parameter λ is real, large and positive. The integration in (18) is over complex-valued slowness surface $S(\mathrm{p})$. The stationary point p_0 on $S(\mathrm{p})$ is defined by

$$\left.\frac{\partial\theta(\mathrm{p})}{\partial s_1}\right|_{\mathrm{p}=\mathrm{p}_0}=0,\quad \left.\frac{\partial\theta(\mathrm{p})}{\partial s_2}\right|_{\mathrm{p}=\mathrm{p}_0}=0\ . \tag{24}$$

where s_1 and s_2 are the complex-valued local coordinates defined on $S(\mathrm{p})$. The third complex-valued coordinate axis s_3 is normal to the slowness surface at p_0 and parallel to N. Since N is a real-valued vector, the s_3-axis is homogeneous. Consequently, the energy velocity vector,

$$\mathrm{v}=v\mathrm{N}=\frac{1}{2}\left.\frac{\partial G}{\partial \mathrm{p}}\right|_{\mathrm{p}=\mathrm{p}_0} \tag{25}$$

must also be homogenous. Expanding phase function $\theta(\mathrm{p})$ near stationary point p_0, yields

$$\theta(\mathrm{p})=\mathrm{p}_0\cdot\mathrm{N}-\frac{1}{2}\left(K_1 s_1^2+K_2 s_2^2\right), \tag{26}$$

where K_1 and K_2 are the complex-valued principal curvatures of the slowness surface at p_0. Applying the steepest descent method (Ben-Menahem & Singh 1981, Appendix E) to integral (18), we obtain

$$G_{kl}^{\mathrm{asym}}(\mathrm{x},\omega)=\frac{i\omega}{8\pi^2\rho}P_{kl}(\mathrm{p}_0)\sqrt{\frac{2\pi}{i\lambda K_1}}\sqrt{\frac{2\pi}{i\lambda K_2}}\exp\left(i\lambda\theta(\mathrm{p}_0)\right), \tag{27}$$

and finally,

$$G_{kl}^{\mathrm{asym}}(\mathrm{x},\omega)=\frac{1}{4\pi\rho}\frac{g_k g_l}{v\sqrt{|K|}}\frac{1}{r}\exp\left(i\sigma_0+i\omega\mathrm{p}_0\cdot\mathrm{x}\right), \tag{28}$$

where

$$\sigma_0 = -\frac{1}{2}(\varphi_1 + \varphi_2)\ ,\ -\frac{3}{2}\pi \le \varphi_1 < \frac{1}{2}\pi\ ,\ -\frac{3}{2}\pi \le \varphi_2 < \frac{1}{2}\pi\ .$$

Angles φ_1 and φ_2 define the phases of the principal curvatures K_1 and K_2., and $|K|$ is the modulus of the Gaussian curvature $K = K_1 K_2$. All quantities dependent on p in (28) are taken at stationary point p_0. Position vector x, distance r, frequency ω, phase angles φ_1 and φ_2, and density ρ are real-valued; but polarization vector g, Gaussian curvature K, principal curvatures K_1 and K_2, energy velocity v and slowness vector p_0 are complex-valued. Similarly as for elastic media, formula (28) fails in singularities.

Decomposing the energy velocity v into real and imaginary parts, v^R and v^I, the exponential term in (28) becomes

$$\exp(i\omega \mathrm{p}_0 \cdot \mathrm{x}) = \exp\left(i\omega \frac{r}{v}\right) = \exp\left(-\omega A^{\mathrm{ray}} r\right) \exp\left(i\omega \frac{r}{V^{\mathrm{ray}}}\right), \tag{29}$$

where

$$V^{\mathrm{ray}} = \frac{v v^*}{v^R} = \frac{v^R v^R + v^I v^I}{v^R}\ , \tag{30}$$

$$A^{\mathrm{ray}} = -\frac{v^I}{v v^*} = -\frac{v^I}{v^R v^R + v^I v^I}\ . \tag{31}$$

The asterisk in (30-31) indicates a complex conjugate quantity. Consequently, the Green function reads

$$G_{kl}^{\mathrm{asym}}(\mathrm{x},\omega) = \frac{i}{4\pi\rho} \frac{g_k g_l}{v\sqrt{|K|}} \frac{\exp\left(-\omega A^{\mathrm{ray}} r\right)}{r} \exp\left(i\sigma_0 + i\omega \frac{r}{V^{\mathrm{ray}}}\right)\ . \tag{32}$$

Since V^{ray} and A^{ray} control the propagation velocity and attenuation along a ray, I shall refer to them as the ray velocity and ray attenuation, respectively.

5. NUMERICAL PROCEDURE

5.1. Stationary point

Determining stationary point p_0 is the crucial and most complicated step in calculating the asymptotic quantities in anisotropic viscoelastic media. Although the exact Green function (11-13) is calculated as a superposition of homogeneous plane waves, the asymptotic Green function is calculated at a stationary point which corresponds to an inhomogeneous plane wave. Hence, the slowness direction at the stationary point is no longer real-valued but it is generally complex-valued.

The complex-valued stationary point p_0 can be determined either by iterations or by solving a system of polynomial equations. The iterative procedure is fast and works well provided the wave front is free of triplications. The procedure is based on seeking a complex-valued slowness direction n_0, for which energy velocity v is homogeneous and points along a specified ray vector N. This represents an inversion for four unknown angles: two angles define the real part and two others define the imaginary part of n_0. We can consider the modulus of the complex-valued deviation between the given and predicted ray vectors as the misfit function. The inversion is non-linear and can be performed using standard methods (Press *et al.* 2002). If the wave front displays triplications, the determination of stationary slowness p_0 is more involved. When using iterations, we have to be careful to find all slowness vectors corresponding to a given ray, which may sometimes be tricky. The other possibility is to follow Vavryčuk (2006a) and solve a system of polynomial equations for the unknown components of p_0.

5.2. Principal curvatures of the slowness surface

The principal curvatures of the slowness surface K_1 and K_2 can conveniently be calculated using the wave-metric tensor H (Vavryčuk 2003, eq. 9)

$$H_{ij} = \frac{1}{2}\frac{\partial^2 G}{\partial p_i \partial p_j} = \frac{\partial v_i}{\partial p_j} \ , \tag{33}$$

which is expressed for the *P* wave as follows (Vavryčuk 2003, eq 17):

$$H_{il}^{(1)} = a_{ijkl} g_j^{(1)} g_k^{(1)} + \frac{v_i^{(12)} v_l^{(12)}}{G^{(1)} - G^{(2)}} + \frac{v_i^{(13)} v_l^{(13)}}{G^{(1)} - G^{(3)}} \ , \tag{34}$$

$$v_i^{(MN)} = a_{ijkl} p_l \left(g_j^{(M)} g_k^{(N)} + g_j^{(N)} g_k^{(M)} \right) , \tag{35}$$

$$G^{(M)} = a_{ijkl} p_i p_l g_j^{(M)} g_k^{(M)} \ , \tag{36}$$

where superscripts *M* and *N* denote the type of wave (*P*, *S*1 or *S*2). The wave-metric tensors of the *S*1 or *S*2 waves are analogous (see Vavryčuk 2003, eqs 18-19). The diagonal form of H reads (Klimeš 2002):

$$\mathrm{H}^{\mathrm{diag}} = v \begin{bmatrix} K_1 & & \\ & K_2 & \\ & & v \end{bmatrix} , \tag{37}$$

hence principal curvatures K_1 and K_2 can directly be calculated from the eigenvalues of H. Subsequently, Gaussian curvature *K* is calculated as (Klimeš 2002, eq. 45)

$$K = \frac{1}{v^4} \det\left(H_{il}\right) . \tag{38}$$

The formulas for the principal and Gaussian curvatures work safely in all directions except for singularities, in which $G^{(1)} = G^{(2)}$ or $G^{(1)} = G^{(3)}$. In such directions and in their close vicinity, equation (34) fails.

7. EXAMPLES

In this section, the derived formulas are validated on numerical examples. First, the formulas are checked against simple closed-form solutions. Second, the formulas are

applied to exemplify the properties of the Green function in realistic anisotropic viscoelastic materials.

7.1. Test models

For isotropic and some simple anisotropic media, the Green function can be expressed in closed form. The existing closed-form solutions have been derived for elastic media, but they can simply be generalized to be applicable also to viscoelastic media (see Appendices A and B). Subsequently, the viscoelastic closed-form Green functions can be used to verify the derived formulas and to test numerical codes.

I adopted two viscoelastic and two elastic test models. The first viscoelastic model is isotropic with parameters in the Voigt notation: $a_{11} = 30 - 1.5i$, $a_{44} = 10 - 0.5i$, and with density $\rho = 1$, and the second viscoelastic model is transversely isotropic with parameters: $a_{11} = a_{22} = a_{33} = 25 - 2.5i$, $a_{44} = a_{55} = 10 - i$, $a_{66} = 4 - 0.4i$, $a_{12} = a_{11} - 2a_{66}$, $a_{13} = a_{23} = a_{11} - 2a_{44}$, and with density $\rho = 1$. The elastic models are described by real parts of the above viscoelastic parameters. The circular frequency ω of the wave field equals 1.

For the four models, I calculated the exact Green function by direct numerical calculation of integrals (12-13), an asymptotic Green function (28), and the exact and far-field analytical Green functions using (A1) and (B3). Figures 1 and 2 show the Green functions in both the elastic and viscoelastic models. The exact solution obtained using the numerical integration coincides with the analytical solution within the width of the line. Similarly, the asymptotic solution perfectly coincides with the analytic far-field approximation. This validates the formulas derived as well as the codes developed.

7.2. Real models

The Green function is calculated in two anisotropic viscoelastic materials: Clay shale and Carbon-epoxy composite (see Tab. 1). The materials display anisotropy in velocities as well as in attenuation. The values for the Clay shale were taken from Carcione & Cavallini (1995) and those for the Carbon-epoxy composite from Hosten *et al.* (1987). The values were slightly modified to make the models transversely isotropic (see Tab. 2).

Figure 3 shows the basic properties of the *P* waves propagating in the materials studied: the left-hand plots show the directional dependence of ray velocity V^{ray} and real-

valued phase velocity V^{phase}, the right-hand plots show the directional dependence of ray attenuation A^{ray} and of phase attenuation A^{phase}. The ray velocity and ray attenuation characterize the propagation velocity and attenuation along a ray, the phase velocity and phase attenuation characterize the propagation velocity and attenuation along the normal to the plane wave front. The magnitudes of the phase quantities are calculated from the complex-valued slowness vector p as

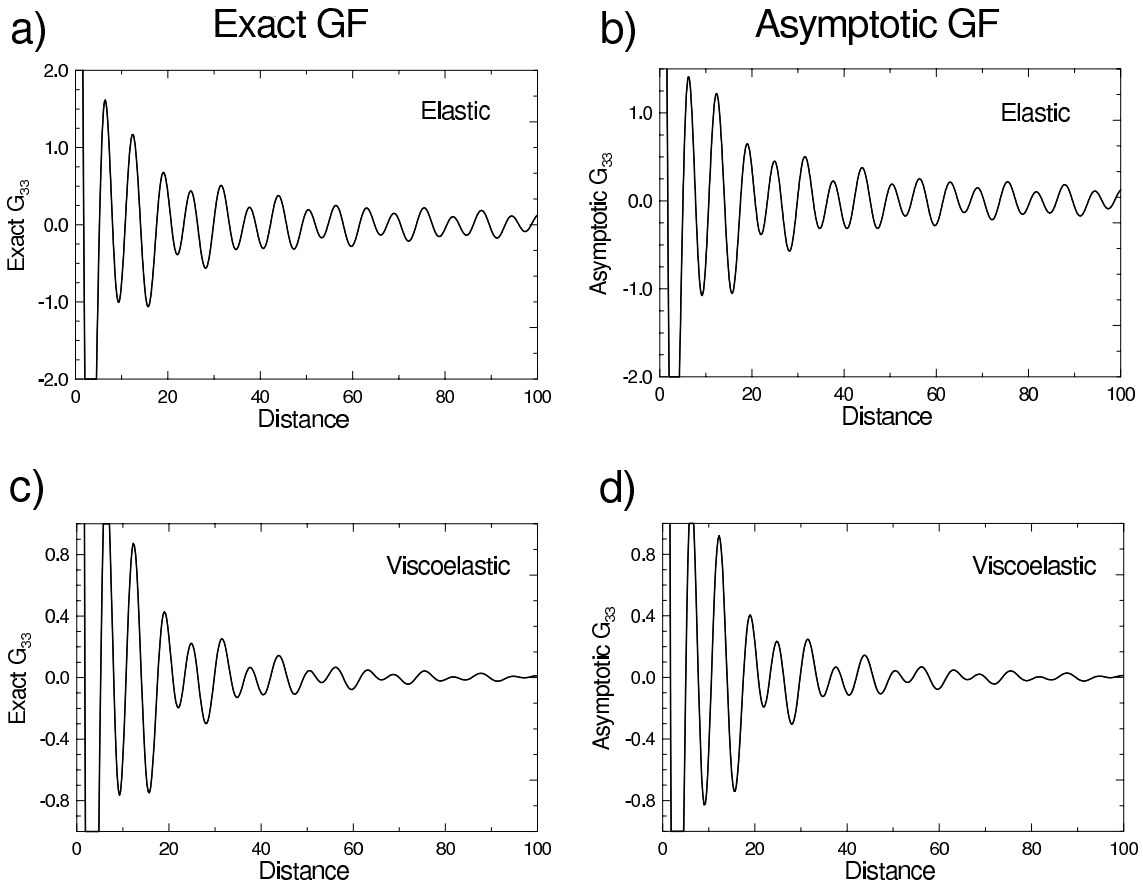

Figure 1. The real part of the G_{33} component of the Green function for an isotropic elastic (a-b) and viscoelastic (c-d) medium. The exact Green function in (a) and (c) is calculated using eq. (11-13) and compared with the closed-form solution (A1). The asymptotic Green function in (b) and (d) is calculated using (28) and compared with the far-field term of solution (A1). The distance is normalized to $\sqrt{a_{44}^R}/\omega$. The Green functions are calculated for a ray deviating by angle $\theta = 45°$ from the vertical.

$$V^{\text{phase}} = \frac{1}{\sqrt{\mathrm{p}^R \cdot \mathrm{p}^R}}, \qquad A^{\text{phase}} = \frac{\mathrm{p}^I \cdot \mathrm{p}^R}{\sqrt{\mathrm{p}^R \cdot \mathrm{p}^R}}, \tag{39}$$

and their direction is along the normal to the plane wave front,

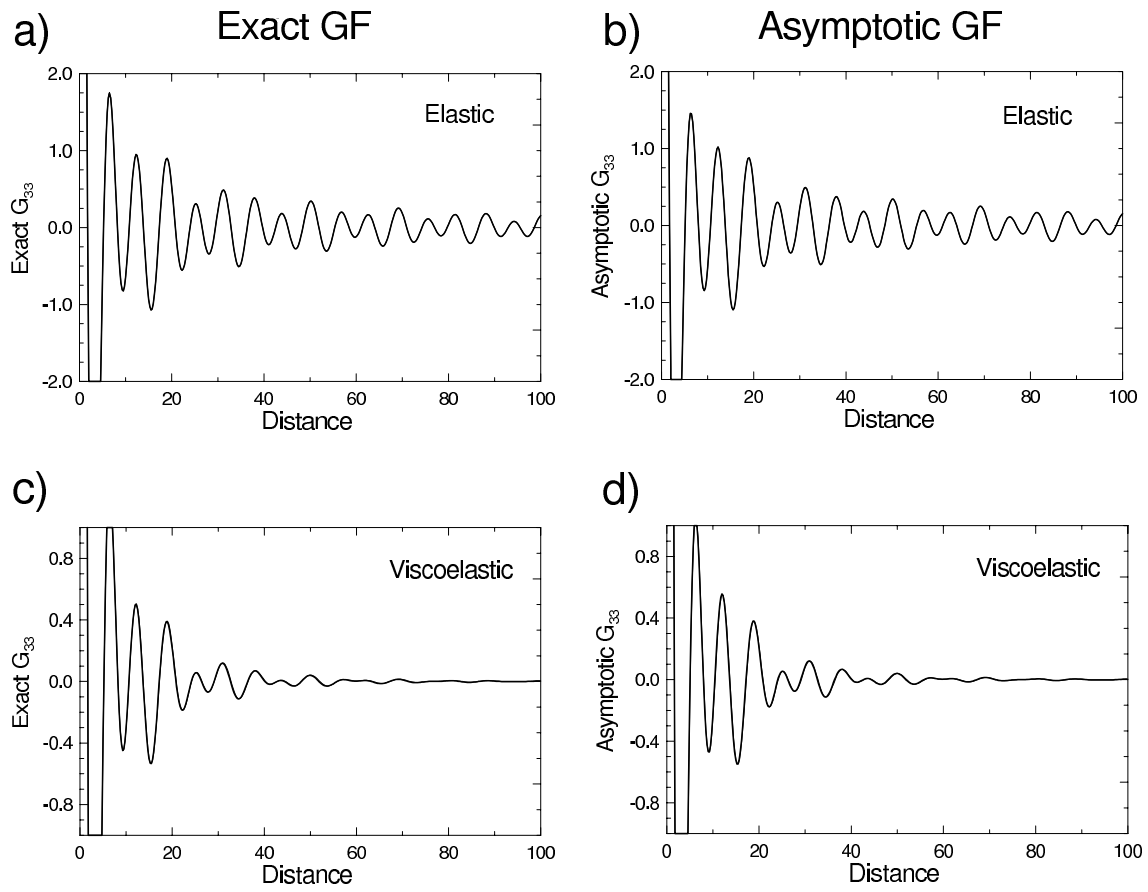

Figure 2. The real part of the G_{33} component of the Green function for a transversely isotropic elastic (a-b) and viscoelastic (c-d) medium. The exact Green function in (a) and (c) is calculated using eq. (11-13) and compared with the closed-form solution (B3). The asymptotic Green function in (b) and (d) is calculated using (28) and compared with the far-field term of solution (B3). The distance is normalized to $\sqrt{a_{44}^R}/\omega$. The Green functions are calculated for a ray deviating by angle $\theta = 45°$ from the vertical.

$$\mathrm{n}^{\mathrm{phase}} = \frac{\mathrm{p}^R}{\sqrt{\mathrm{p}^R \cdot \mathrm{p}^R}}. \tag{40}$$

The magnitudes of the ray quantities are defined by (30-31) and they point along ray vector N. Emphasize that slowness vector p is stationary for both the ray and phase quantities, hence it is, in general, an inhomogeneous complex-valued vector. The corresponding energy velocity vector v must be homogeneous, and ray vector $\mathrm{N} = \mathrm{v}/v$ is real-valued.

Figure 4 shows a comparison of the exact and asymptotic *P*-wave Green functions for the two materials studied. The figure indicates that the asymptotic Green function approximates the exact Green function quite efficiently. As expected, the fit improves with increasing distance from the source. At distance of 15 wavelengths from the source the error in the modulus of the asymptotic Green function is about 4% or less for all 4 examples in Fig. 4.

Table 1. Visocelastic parameters

Elastic parameters						
Model	c_{11}^R [GPa]	c_{13}^R [GPa]	c_{33}^R [GPa]	c_{44}^R [GPa]	c_{66}^R [GPa]	ρ [kg/m^3]
Clay shale	68.7	40.1	42.0	11.4	24.2	2590
Carbon-epoxy	15.0	3.4	87.0	7.8	3.9	1595
Q-factors						
Model	Q_{11}	Q_{13}	Q_{33}	Q_{44}	Q_{66}	f [Hz]
Clay shale	29.7	52.8	18.2	20.3	31.1	20
Carbon-epoxy	34.1	2.4	5.4	59.1	36.5	$5 \cdot 10^6$

Matrix of quality factors Q is defined as $Q_{KL} = -c_{KL}^R / c_{KL}^I$, $K, L = 1,\ldots,6$. The two-index Voigt notation is used for viscoelastic parameters. The Clay shale model is taken from Carcione & Cavallini (1995b), the Carbon-epoxy model is from Hosten *et al.* (1987).

Table 2. *P*-wave anisotropy of velocity and attenuation

Model	$\overline{V}^{\text{ray}}$ [10^3 m/s]	a_V^{ray} [%]	$\overline{A}^{\text{ray}}$ [10^{-7} s/m]	a_Q^{ray} [%]
Clay shale	4.63	24.4	46.7	71.0
Carbon-epoxy	4.35	83.7	81.1	88.0

$\overline{V}^{\text{ray}}$ is the mean *P*-wave ray velocity, a_V^{ray} the *P*-wave velocity anisotropy, $\overline{A}^{\text{ray}}$ the mean *P*-wave ray attenuation and a_Q^{ray} the *P*-wave ray attenuation anisotropy. The velocity and attenuation anisotropy is calculated as $a_V^{\text{ray}} = 200\left(V_{\text{MAX}}^{\text{ray}} - V_{\text{MIN}}^{\text{ray}}\right)/\left(V_{\text{MAX}}^{\text{ray}} + V_{\text{MIN}}^{\text{ray}}\right)$, $a_Q^{\text{ray}} = 200\left(A_{\text{MAX}}^{\text{ray}} - A_{\text{MIN}}^{\text{ray}}\right)/\left(A_{\text{MAX}}^{\text{ray}} + A_{\text{MIN}}^{\text{ray}}\right)$, where subscripts MAX and MIN indicate the maximum and minimum values over all rays.

8. CONCLUSION

The exact Green function in homogeneous anisotropic viscoelastic media is calculated as in elastic media by numerically integrating a surface and line integrals. The surface integral defines the regular part of the Green function, and physically corresponds to a superposition of homogeneous plane waves. The line integral defines the singular part of the Green function. While all quantities in the integrals are real-valued in elastic media, some of them become complex-valued in viscoelastic media. However, this difference is minor and does not pose complications to computing the Green function. The complex-valued integrals can be calculated either directly using numerical integration or asymptotically using the steepest-descent method. In some very simple cases, the integrals can also be calculated analytically yielding closed-form solutions.

The calculation of the asymptotic Green function is more involved in viscoelastic media than in elastic media. Although the exact Green function in viscoelastic media is calculated as a superposition of homogeneous plane waves, the asymptotic Green function is calculated at a stationary point which corresponds to an inhomogeneous plane wave. In elastic media, we usually start with setting a slowness vector and then calculate the corresponding ray direction. The slowness vector is always homogeneous. In viscoelastic

media, we first define the ray direction and seek the slowness vector that predicts the vector of the energy velocity parallel to the ray. Since the ray direction is real, the energy velocity vector is homogeneous. Consequently, the stationary slowness vector is, in general, inhomogeneous and its computation involves finding two independent unit vectors, which specify the directions of its real and imaginary parts. This can be done iteratively in a simple way, provided the wave surface is free of triplications. If not, we have to take care of getting all slowness vectors corresponding to a given ray, or we solve a system of polynomial equations.

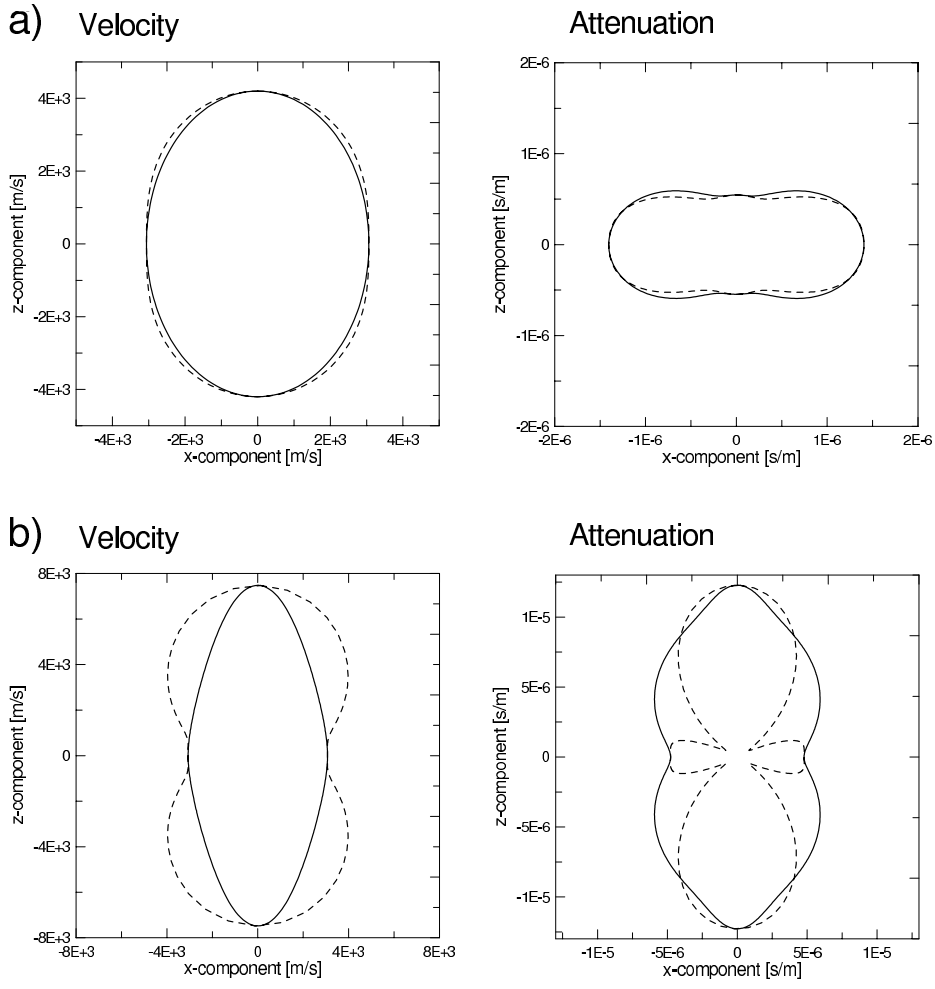

Figure 3. The *P*-wave velocity and attenuation in Clay shale (a) and Carbon/epoxy composite (b). The left-hand plots show the directional dependence of ray and phase velocities, the right-hand plots show a directional dependence of the ray and phase attenuations. The solid line denotes the ray quantities, the dashed line denotes the phase quantities.

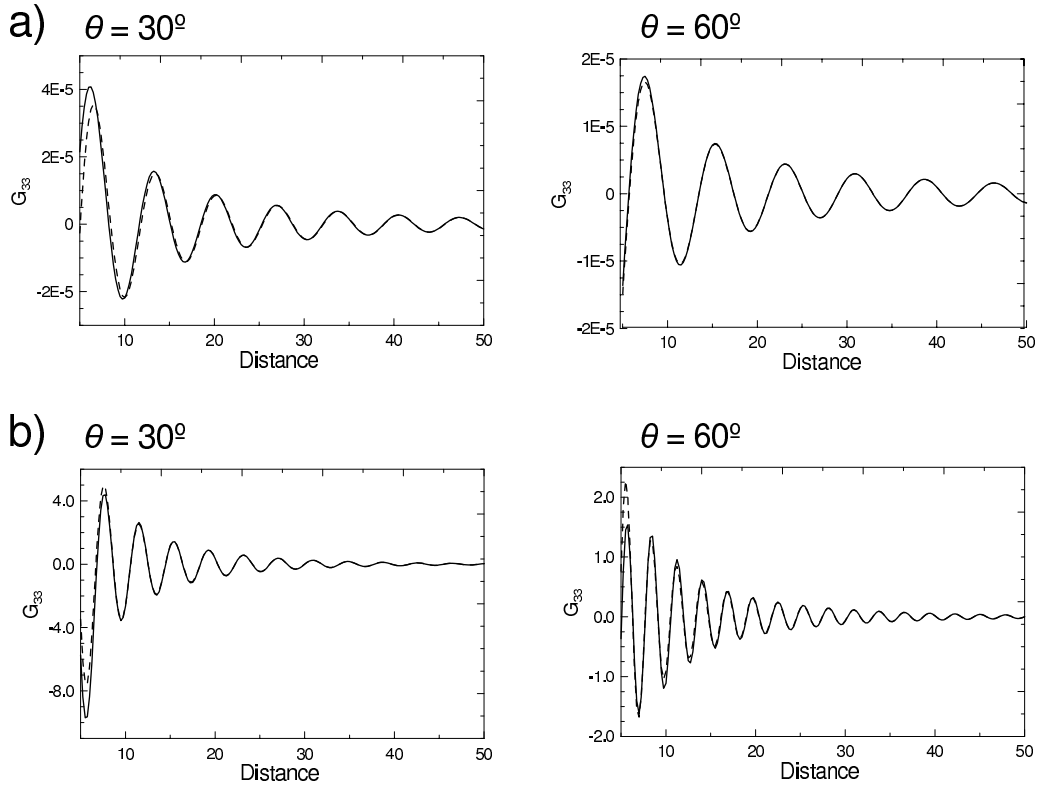

Figure 4. The real part of the G_{33} component of the exact and asymptotic *P*-wave Green function in Clay shale (a) and in Carbon/epoxy composite (b). The solid line shows the exact Green function calculated using eq. (11-13), the dashed line shows the asymptotic Green function calculated using eq. (28). The Green functions are for a ray deviating from the vertical by angle $\theta = 30°$ (left-hand plots) and $\theta = 60°$ (right-hand plots). The distance is normalized to $\sqrt{a_{33}^R}/\omega$. The Green function is in 10^{-10} m/s.

ACKNOWLEDGEMENTS

I thank Colin Thomson for discussions on the subject, and Klaus Helbig and two anonymous referees for their comments. This work was supported by the Grant Agency of the Czech Republic, Grant No. 205/05/2182 and by the Consortium Project SW3D "Seismic Waves in Complex 3-D Structures".

REFERENCES

Aki, K., & Richards, P.G., 2002. *Quantitative Seismology*. University Science Books, Sausalito, California.

Auld, B.A., 1973. *Acoustic Fields and Waves in Solids*. Wiley, New York.

Ben-Menahem, A., & Singh, S.J., 1981. *Seismic Waves and Sources*. Springer-Verlag, New York.

Borcherdt, R.D., 1977. Reflection-refraction of type-II S waves in elastic and anelastic media. *Bull. Seism. Soc. Am.* 67, 43-67.

Borcherdt, R.D., 1982. Reflection-refraction of general P- and type-I S waves in elastic and anelastic solids. *Geophys. J. R. Astr. Soc.* 70, 621-638.

Boulanger, P., 1998. Energy flux for damped inhomogeneous plane waves in viscoelastic fluids. *Wave Motion* 28, 215-225.

Buchwald V.T., 1959. Elastic waves in anisotropic media. *Proc. R. Soc. Lond. A* 253, 563-580.

Burridge R., 1967. The singularity on the plane lids of the wave surface of elastic media with cubic symmetry. *Q. J. Mech. appl. Math.* 20, 41-56.

Burridge, R., Chadwick, P., & Norris, A.N., 1993. Fundamental elastodynamic solutions for anisotropic media with ellipsoidal slowness surfaces. *Pros. R. Soc. Lond. A* 440, 655-681.

Brokešová, J., 2001. Reflection/transmission coefficients at a plane interface in dissipative and nondissipative isotropic media: a comparison. *J. Comput. Acoustics* 9, 623-641.

Carcione, J.M., 1990. Wave propagation in anisotropic linear viscoelastic media: theory and simulated wavefields *Geophys. J. Int.* 101, 739-750. Erratum: 1992, 111, 191.

Carcione, J.M, 1994. Wavefronts in dissipative anisotropic media. *Geophysics* 59, 644-657.

Carcione, J.M., 2001. *Wave Fields in Real Media: Wave Propagation in Anisotropic, Anelastic and Porous Media.* Pergamon, Amsterdam.

Carcione, J.M., & Cavallini, F., 1993. Energy balance and fundamental relations in anisotropic-viscoelastic media. *Wave Motion* 18, 11-20.

Carcione, J.M., & Cavallini, F., 1995. Attenuation and quality factor surfaces in anisotropic-viscoelastic media. *Mech. Mat.* 19, 311-327.

Caviglia, G., & Morro, A., 1992. *Inhomogeneous Waves in Solids and Fluids*. World Scientific.

Červený, V., 2001. *Seismic Ray Theory*. Cambridge University Press, Cambridge, U.K.

Červený, V., & Pšenčík, I., 2005. Plane waves in viscoelastic anisotropic media – I. Theory. *Geophys. J. Int*. 161, 197-212, doi:10.1111/j.1365-246X.2005.02589.x.

Červený, V., & Pšenčík, I., 2006. Energy flux in viscoelastic anisotropic media. *Geophys. J. Int*. 166, 1299-1317, doi:10.1111/j.1365-246X.2006.03057.x.

Daley, P.F., & Krebes, E.S., 2004. SH wave propagation in viscoelastic media. *Stud. Geophys. Geod.* 48, 563-587, 10.1023/B:SGEG.0000037472.40481.cd.

Deschamps, M., Poirée, B., & Poncelet, O., 1997. Energy velocity of complex harmonic plane waves in viscous fluids. *Wave Motion* 25, 51-60.

Every A.G. and Kim K.Y., 1994: Time domain dynamic response functions of elastically anisotropic solids. *J. Acoust. Soc. Am.* 95, 2505-2516.

Gridin D., 2000. Far-field asymptotics of the Green tensor for a transversely isotropic solid. *Proc. R. Soc. Lond. A* 456, 571-591.

Hosten, B., Deschamps, M., & Tittmann, B.R., 1987. Inhomogeneous wave propagation in lossy anisotropic solids. Application to the characterization of viscoelastic composite materials. *J. Acoust. Soc. Am.* 82, 1763-1770.

Klimeš, L., 2002. Relation of the wave-propagation metric tensor to the curvatures of the slowness and ray-velocity surfaces. *Stud. Geophys. Geod.* 46, 589–597, doi: 10.1023/A:1019551320867.

Krebes, E.S., 1983. The viscoelastic reflection/transmission problem: two special cases. *Bull. Seism. Soc. Am.* 73, 1673-1683.

Moczo, P., Robertsson, J.O.A., & Eisner, L., 2007. The Finite-Difference Time-Domain Method for Modelling of Seismic Wave Propagation. In *Advances in Wave Propagation in Heterogeneous Earth*, 421-516, Wu, R.-S., Maupin, V., eds., Advances in Geophysics 48, Dmowska, R., ed., Elsevier – Academic Press, doi: 10.1016/S0065-2687(06)48008-0.

Mura, T., 1987. *Micromechanics of Defects in Solids*, 2nd ed., Martinus Nijhoff, Dordrecht.

Nechtschein, S., & Hron, F., 1996. Reflection and transmission coefficients between two anelastic media using asymptotic ray theory. *Can. J. Expl. Geophys*. 32, 31-40.

Norris, A.N., 1994. Dynamic Green's functions in anisotropic piezoelectric, thermoelastic and poroelastic solids. *Proc. R. Soc. Lond. A.* 447, 175-188.

Payton, R.G., 1983. *Elastic Wave Propagation in Transversely Isotropic Media*. Martinus Nijhoff Publishers, The Hague.

Press, W.H., Teukolsky, S.A., Vetterling, W.T., Flannery, B.P., 2002. *Numerical Recipes: The Art of Scientific Computing*. Cambridge University Press.

Richards, P.G., 1984. On wavefronts and interfaces in anelastic media. *Bull. Seism. Soc. Am.* 74, 2157-2165.

Saenger, E.H., & Bohlen, T., 2004. Finite-difference modeling of viscoelastic and anisotropic wave propagation using the rotated staggered grid. *Geophysics* 69, 583-591, doi:10.1190/1.1707078.

Shuvalov, A.L., 2001. On the theory of plane inhomogeneous waves in anisotropic elastic media. *Wave Motion* 34, 401-429.

Shuvalov, A.L., & Scott, N.H., 1999. On the properties of homogeneous viscoelastic waves. *Q. J. Mech. Appl. Math* 52, 405-417.

Vavryčuk, V., 1999. Properties of S waves near a kiss singularity: a comparison of exact and ray solutions, *Geophys. J. Int.* 138, 581-589, doi:10.1046/j.1365-246X.1999.00887.x.

Vavryčuk, V., 2001. Exact elastodynamic Green functions for simple types of anisotropy derived from higher-order ray theory. *Stud. Geophys. Geod.* 45, 67-84, doi: 10.1023/A:1021754530968.

Vavryčuk, V., 2002. Asymptotic elastodynamic Green function in the kiss singularity in homogeneous anisotropic solids. *Stud. Geophys. Geod.* 46, 249-266, doi: 10.1023/A:1019854020095.

Vavryčuk, V., 2003. Parabolic lines and caustics in homogeneous weakly anisotropic solids. *Geophys. J. Int.* 152, 318-334, doi:10.1046/j.1365-246X.2003.01845.x.

Vavryčuk, V., 2006a. Calculation of the slowness vector from the ray vector in anisotropic media. *Proc. R. Soc. A* 462, 883-896, doi: 10.1098/rspa.2005.1605.

Vavryčuk, V., 2006b. Comment to "qS-waves in a vicinity of the axis of symmetry of homogeneous transversely isotropic media", by M. Popov, G.F. Passos, and M.A. Botelho [Wave Motion 42 (2005) 191-201]. *Wave Motion* 44, 128-136, doi:10.1016/j.wavemoti.2006.08.004.

Wang, C.-Y., & Achenbach, J.D., 1994. Elastodynamic fundamental solutions for anisotropic solids. *Geophys. J. Int.* 118, 384-392.

Wennerberg, L., 1985. Snell's law for viscoelastic materials. *Geophys. J. Roy. Astr. Soc.* 81, 13-18.

Willis, J.R., 1980. A polarization approach to the scattering of elastic waves. I. Scattering by a single inclusion. *J. Mech. Phys. Solids* 28, 287-305.

Zhu, Y., & Tsvankin, I., 2006. Plane-wave propagation in attenuative transversely isotropic media. *Geophysics* 71 (2), T17-T30, doi:10.1190/1.2187792.

Zhu, Y., & Tsvankin, I., 2007. Plane-wave attenuation anisotropy in orthorhombic media. *Geophysics* 72 (1), D9-D19, doi:10.1190/1.2387137.

APPENDIX A: GREEN FUNCTION IN AN ISOTROPIC VISCOELASTIC MEDIUM

Solving integrals (12) and (13) for a homogeneous isotropic viscoelastic medium, we arrive at the exact viscoelastic Green function in a form quite analogous to that for an elastic medium (Aki & Richards, 2002, eq. 4.35). Hence,

$$G_{kl}^{\text{exact}}(\mathrm{x},\omega) = G_{kl}^{\text{near}}(\mathrm{x},\omega) + G_{kl}^{\text{far}}(\mathrm{x},\omega) \ ,$$

$$G_{kl}^{\text{near}}(\mathrm{x},\omega) = \frac{3N_kN_l - \delta_{kl}}{4\pi\rho r}\left\{\frac{1}{\alpha^2}\exp\left(i\omega\frac{r}{\alpha}\right)\left[\left(-\frac{\alpha}{i\omega r}\right)+\left(-\frac{\alpha}{i\omega r}\right)^2\right] - \frac{1}{\beta^2}\exp\left(i\omega\frac{r}{\beta}\right)\left[\left(-\frac{\beta}{i\omega r}\right)+\left(-\frac{\beta}{i\omega r}\right)^2\right]\right\} \tag{A1}$$

$$G_{kl}^{\text{far}}(\mathrm{x},\omega) = \frac{1}{4\pi\rho r}\left\{\frac{N_kN_l}{\alpha^2}\exp\left(i\omega\frac{r}{\alpha}\right) - \frac{N_kN_l - \delta_{kl}}{\beta^2}\exp\left(i\omega\frac{r}{\beta}\right)\right\},$$

where $G_{kl}^{\text{near}}(\mathrm{x},\omega)$ and $G_{kl}^{\text{far}}(\mathrm{x},\omega)$ are the near-field and far-field terms of the Green function, respectively. Vector N is the ray direction, δ_{kl} the Kronecker delta, ρ the density of the medium, r the distance, and $\alpha = \sqrt{a_{11}}$ and $\beta = \sqrt{a_{44}}$ are the velocities of the P and S waves. All quantities in (A1) are real-valued except for the complex-valued velocities α and β.

APPENDIX B: GREEN FUNCTIONS IN SIMPLE ANISOTROPIC VISCOELASTIC MEDIA

Here I mention Green functions in a closed form for three simple types of anisotropy. The first anisotropy displays an orthorhombic symmetry, the other two types display transverse isotropy. In all cases, the complex-valued slowness surfaces of waves are either ellipsoids, spheroids or spheres. The viscoelastic Green functions are obtained by expressing the elastic Green functions in the frequency domain, and by substituting the real-valued elastic parameters by complex-valued viscoelastic parameters. The elastic Green functions have been published by Payton (1983), Burridge *et al.* (1993) and by Vavryčuk (2001).

Anisotropy I

Let us consider an orthorhombic medium with the following density normalized viscoelastic coefficients: a_{11}, a_{22}, a_{33}, a_{44}, a_{55}, a_{66}, $a_{12}=-a_{66}$, $a_{13}=-a_{55}$, $a_{23}=-a_{44}$, the other coefficients being zero. The exact formula for the Green function reads

$$G_{kl}^{\text{exact}}(\mathrm{x},\omega)=\frac{1}{4\pi\rho}\left\{\frac{\delta_{k1}\delta_{l1}}{\sqrt{a_{11}a_{55}a_{66}}}\frac{\exp\left(i\omega\tau^{(1)}\right)}{\tau^{(1)}}+\frac{\delta_{k2}\delta_{l2}}{\sqrt{a_{22}a_{44}a_{66}}}\frac{\exp\left(i\omega\tau^{(2)}\right)}{\tau^{(2)}}+\frac{\delta_{k3}\delta_{l3}}{\sqrt{a_{33}a_{44}a_{55}}}\frac{\exp\left(i\omega\tau^{(3)}\right)}{\tau^{(3)}}\right\} \tag{B1}$$

where

$$\tau^{(1)}=r\sqrt{\frac{N_1^2}{a_{11}}+\frac{N_2^2}{a_{66}}+\frac{N_3^2}{a_{55}}},\quad \tau^{(2)}=r\sqrt{\frac{N_1^2}{a_{66}}+\frac{N_2^2}{a_{22}}+\frac{N_3^2}{a_{44}}},\quad \tau^{(3)}=r\sqrt{\frac{N_1^2}{a_{55}}+\frac{N_2^2}{a_{44}}+\frac{N_3^2}{a_{33}}},$$

are travel times, r is the distance, δ_{kl} the Kronesker delta, and $\mathrm{N}=\frac{\mathrm{x}}{r}$ the ray direction. All quantities in (B1) are real-valued except for the complex-valued viscoelastic parameters a_{ij} and travel times τ.

Green function (B1) is probably the simplest Green function, which can be found in anisotropic viscoelastic media. It consists of the far-field terms only. No near-field terms

and no effects connected to intersection singularities, which are present in the wave field, are observed.

Anisotropy II

Let us consider a transversely isotropic medium with a vertical axis of symmetry and with the following density-normalized viscoelastic coefficients: a_{11}, $a_{22}=a_{11}$, a_{33}, a_{44}, $a_{55}=a_{44}$, a_{66}, $a_{12}=a_{11}-2a_{66}$, $a_{13}=-a_{44}$, $a_{23}=-a_{44}$, the other coefficients being zero. The exact formula for the Green function reads

$$G_{kl}^{\text{exact}}(\mathrm{x},\omega)=G_{kl}^{\text{near}}(\mathrm{x},\omega)+G_{kl}^{\text{far}}(\mathrm{x},\omega)\,,$$

$$G_{kl}^{\text{near}}(\mathrm{x},\omega)=\frac{1}{4\pi\rho\sqrt{a_{44}}}\frac{g_k^{(2)}g_l^{(2)}-g_k^{(3)}g_l^{(3)}}{R^2}\left(\frac{-1}{i\omega}\right)\left[\exp\left(i\omega\tau^{(3)}\right)-\exp\left(i\omega\tau^{(2)}\right)\right], \tag{B2}$$

$$G_{kl}^{\text{far}}(\mathrm{x},\omega)=\frac{1}{4\pi\rho}\left\{\frac{g_k^{(1)}g_l^{(1)}}{a_{44}\sqrt{a_{33}}}\frac{\exp\left(i\omega\tau^{(1)}\right)}{\tau^{(1)}}+\frac{g_k^{(2)}g_l^{(2)}}{a_{11}\sqrt{a_{44}}}\frac{\exp\left(i\omega\tau^{(2)}\right)}{\tau^{(2)}}+\frac{g_k^{(3)}g_l^{(3)}}{a_{66}\sqrt{a_{44}}}\frac{\exp\left(i\omega\tau^{(3)}\right)}{\tau^{(3)}}\right\}\,,$$

where

$$\tau^{(1)}=\frac{r}{\sqrt{a_{44}}}\sqrt{N_1^2+N_2^2+\frac{a_{44}}{a_{33}}N_3^2}\,,\quad \tau^{(2)}=\frac{r}{\sqrt{a_{11}}}\sqrt{N_1^2+N_2^2+\frac{a_{11}}{a_{44}}N_3^2}\,,$$

$$\tau^{(3)}=\frac{r}{\sqrt{a_{66}}}\sqrt{N_1^2+N_2^2+\frac{a_{66}}{a_{44}}N_3^2}\,,$$

are travel times,

$$\mathrm{g}^{(1)}=\begin{bmatrix}0\\0\\1\end{bmatrix}\,,\ \mathrm{g}^{(2)}=\frac{1}{\sqrt{N_1^2+N_2^2}}\begin{bmatrix}N_1\\N_2\\0\end{bmatrix}\,,\ \mathrm{g}^{(2)}=\frac{1}{\sqrt{N_1^2+N_2^2}}\begin{bmatrix}N_2\\-N_1\\0\end{bmatrix}\,,$$

are polarization vectors, r is the distance of the observation point from the source, $R=\sqrt{x_1^2+x_2^2}$ the distance of the observation point from the symmetry axis, and $\mathrm{N}=\frac{\mathrm{x}}{r}$ is the ray direction. All quantities in (B2) are real-valued except for complex-valued viscoelastic parameters a_{ij} and travel times τ.

The Green function (B2) consists of the far-field term as well as of the near-singularity term (see Vavryčuk 1999). The near-singularity term is significant near the symmetry axis, where a kiss singularity is observed. The amplitude of this term decreases with distance R from the singularity as $1/R^2$. Physically, the near-singularity term represents the coupling between the *SV* and *SH* waves (Vavryčuk 1999, 2006b).

Anisotropy III

Let us consider a transversely isotropic medium with a vertical axis of symmetry and with the following density-normalized viscoelastic coefficients: a_{11}, $a_{22}=a_{11}$, $a_{33}=a_{11}$, a_{44}, $a_{55}=a_{44}$, a_{66}, $a_{12}=a_{11}-2a_{66}$, $a_{13}=a_{11}-2a_{44}$, $a_{23}=a_{11}-2a_{44}$, the other coefficients being zero. The exact formula for the Green function reads

$$G_{kl}^{\mathrm{exact}}(\mathrm{x},\omega)=G_{kl}^{\mathrm{near}}(\mathrm{x},\omega)+G_{kl}^{\mathrm{far}}(\mathrm{x},\omega)\,,$$

$$G_{kl}^{\mathrm{near}}(\mathrm{x},\omega)=\frac{1}{4\pi\rho\sqrt{a_{44}}}\frac{g_k^{(3)\perp}g_l^{(3)\perp}-g_k^{(3)}g_l^{(3)}}{R^2}\left(\frac{-1}{i\omega}\right)\left[\exp\left(i\omega\tau^{(3)}\right)-\exp\left(i\omega\tau^{(2)}\right)\right]$$
$$+\frac{3g_k^{(1)}g_l^{1}-\delta_{kl}}{4\pi\rho r}\left\{\frac{1}{a_{11}}\exp\left(i\omega t^{(1)}\right)\left[\left(\frac{-1}{i\omega\tau^{(1)}}\right)+\left(\frac{-1}{i\omega\tau^{(1)}}\right)^2\right]-\frac{1}{a_{44}}\exp\left(i\omega\tau^{(2)}\right)\left[\left(\frac{-1}{i\omega\tau^{(2)}}\right)+\left(\frac{-1}{i\omega\tau^{(2)}}\right)^2\right]\right\} \tag{B3}$$

$$G_{kl}^{\mathrm{far}}(\mathrm{x},\omega)=\frac{1}{4\pi\rho}\left\{\frac{g_k^{(1)}g_l^{(1)}}{\sqrt{a_{11}^3}}\frac{\exp\left(i\omega\tau^{(1)}\right)}{\tau^{(1)}}+\frac{g_k^{(2)}g_l^{(2)}}{\sqrt{a_{44}^3}}\frac{\exp\left(i\omega\tau^{(2)}\right)}{\tau^{(2)}}+\frac{g_k^{(3)}g_l^{(3)}}{a_{66}\sqrt{a_{44}}}\frac{\exp\left(i\omega\tau^{(3)}\right)}{\tau^{(3)}}\right\}\,,$$

where

$$\tau^{(1)} = \frac{r}{\sqrt{a_{11}}},\ \ \tau^{(2)} = \frac{r}{\sqrt{a_{44}}},\ \tau^{(3)} = \frac{r}{\sqrt{a_{66}}}\sqrt{N_1^2 + N_2^2 + \frac{a_{66}}{a_{44}}N_3^2}\ ,$$

are travel times,

$$\mathrm{g}^{(1)} = \begin{bmatrix} N_1 \\ N_2 \\ N_3 \end{bmatrix},\ \mathrm{g}^{(2)} = \frac{1}{\sqrt{N_1^2 + N_2^2}}\begin{bmatrix} -N_1N_3 \\ -N_2N_3 \\ N_1^2 + N_2^2 \end{bmatrix},\ \mathrm{g}^{(2)} = \frac{1}{\sqrt{N_1^2 + N_2^2}}\begin{bmatrix} N_2 \\ -N_1 \\ 0 \end{bmatrix},$$

are polarization vectors, r is the distance of the observation point from the source, $R = \sqrt{x_1^2 + x_2^2}$ the distance of the observation point from the symmetry axis, and $\mathrm{N} = \frac{\mathrm{x}}{r}$ is the ray direction. All quantities in (B3) are real-valued except for complex-valued viscoelastic parameters a_{ij} and travel times τ.

The Green function (B3) consists of the far-field term as well as the near-field and near-singularity terms. The near-field term represents the coupling between the *P* and *SV* waves and is quite analogous to the near-field term observed in isotropic media (A1). The near-singularity term is significant near the symmetry axis, similarly as in Anisotropy II (B2).